

# SI Appendix

Beilina et al

## Supplementary Materials and Methods

### *Plasmids and cell lines*

Myc- or Flag-tagged LRRK2 and LRRK1<sup>1,2</sup>, Flag-tagged BAG5<sup>3</sup> and GFP-tagged GAK constructs including deletion constructs<sup>4</sup> have been described previously. Full length Rab7L1 was amplified from human cerebral cortex cDNA using PCR primers: 5'-ATGGGCAGCCGCGACCACCT-3' and 5'-CTAGCAGCAGGACCAGCTGG-3'. BAG5 was cloned using: 5'-ATGGATATGGGAAACCAACA-3' and 5'-GTACTCCATTCATCAGATTTC-3'. Full length GAK was amplified with: 5'-ATGTCGCTGCTGCAGTCGGC-3' and 5'-TCAGAAGAGGGGCCGGGAGCCC-3'.

PCR products were purified and cloned into pCR8/GW/TOPO vector (Invitrogen) then transferred into pCMV-2xmyc-DEST<sup>2</sup>, a Gateway-modified p3xFlag-CMV<sup>TM</sup>-7.1 N-terminal Met-3xFlag vector (Sigma), pLenti6/V5-DEST (Invitrogen) using Gateway recombination (Invitrogen). T21N and Q67L Rab7L1 mutations were introduced by the QuikChange II site-directed mutagenesis kit (Stratagene).

### *Protoarrays*

GST-tagged, truncated (970–2527) kinase active LRRK2 was purchased from Invitrogen and used as a probe for initial protein arrays. The GST-LRRK2 protein was first dialyzed against 1x PBS to remove Tris storage buffer and then was concentrated using Centrifugal Filter with 30K membrane (Millipore). Concentrated protein was then labeled using the Biotin-XX Microscale protein labeling kit (Invitrogen). We estimated that ~8 biotin molecules were incorporated per molecule of LRRK2. GST-LRRK2 (970–2527) remained active as a kinase after biotin labeling (**Supplementary Fig. 1**).

Protoarrays, version 4.1 (Invitrogen, Lot number HA20150) were probed with biotinylated LRRK2

according to the manufacturer's instructions. In this version of the arrays, target proteins on the arrays were hybridized with GST tags oriented towards the glass surface. Five arrays were screened in two batches. In the first batch, we used hybridization buffer alone and either used 6 mg of GST or 6 mg GST-LRRK2 to probe the arrays. In the second batch, we probed with 6 mg GST-LRRK2 in the presence of 200 mM GDP and 6 mg GST-LRRK2 in the presence of 200 mM GMPPcP, with both nucleotides included in the hybridization buffer. Protein binding was visualized using streptavidin-AlexaFluor647 conjugate and arrays were imaged using an Axon GenePix 4000B fluorescence scanner.

For full-length LRRK2, we purified Flag-tagged protein or Flag-GFP as a negative control as described previously<sup>1</sup>. Six mg of each purified 3xFlag-LRRK2 and 3xFlag-eGFP proteins were used to probe Protoarrays, version 5.03 (Invitrogen, Lot number HA20265) according to the manufacturer's instructions with the modification that after 3xFlag-tagged protein probing, arrays were probed with monoclonal ANTI-FLAG<sup>®</sup> BioM2–Biotin, Clone M2 (Sigma-Aldrich) antibody, followed by probing with Alexa Fluor<sup>®</sup> 647 streptavidin (Invitrogen). In this version of the arrays, target proteins on the arrays were hybridized randomly with respect to orientation relative to the glass slide.

Raw array images were converted to text files using GenePix Pro that were then used as input into ProtoArray Prospector (Invitrogen). Within ProtoArray Prospector, binding strength was estimated as Z-scores, i.e. numbers of standard deviations above background fluorescence on the array. Each protein on the array is spotted in duplicate, hence reported values are averaged for both spots. To develop a list of candidate interactors for truncated LRRK2, we filtered the

raw data from the first set of experiments to generate a list of proteins that had Z-scores >3 for GST-LRRK2 in all conditions and had Z-scores <3 for both buffer and GST. Similarly, for full-length LRRK2, we filtered the raw data from the second set of arrays for those candidates with Z>3 for LRRK2 and Z<3 for eGFP from the arrays probed in parallel. Because there are differences in manufacture between the two array lots, we did not combine the analyses of the GST-LRRK2 and full-length protein. Raw data, before filtering was applied, is included in the supplementary online material.

#### *Cell culture and transfections*

HEK293FT cells (Invitrogen) were maintained in DMEM (Lonza) containing 4.5 g/l glucose, 2 mM l-glutamine, and 10% fetal bovine serum (Lonza) at 37°C in 5% CO<sub>2</sub>. Transient transfection of cells was performed using PEI (polyethylenimine) (Polysciences) or Lipofectamine 2000 (Invitrogen), according to the manufacturer's instructions. To knockdown endogenous genes, cells were co-transfected with the SMARTpool ON-TARGETplus BAG5, GAK, LRRK2, Rab7L1 or scrambled siRNAs for 48 hours using DharmaFECT transfection reagent (Thermo scientific). Transgene expression in siRNA transfected cells were performed 24 hours after siRNA transfection for additional 24 hours using Lipofectamine 2000 (Invitrogen) or DharmaFECT Duo transfection reagents (Thermo scientific). Primary neurons from cortex were prepared from postnatal day 0 pups and plated onto coverslips precoated with poly-D-lysine (Neuvitro) at 0.7x10<sup>6</sup> cells/well as described<sup>5</sup>. Transfections were performed on day 2 *in vitro* using a modified CaPO<sub>4</sub> method<sup>6</sup>.

#### *Lentiviral transduction and GLG1 staining in mouse brain*

HIV-1 derived lentiviral vector particles encoding eGFP or eGFP-LRRK2 G2019S were generated by the Leuven Viral Vector Core (LVVC), Laboratory for Neurobiology and Gene Therapy, essentially as described<sup>6</sup>. Briefly, after seeding HEK293T cells in 15-cm dishes, we performed a triple transient transfection with the respective

transfer plasmids, a packaging plasmid and an envelope plasmid encoding VSV G. The production was performed in Opti-MEM I (Gibco-Invitrogen, Merelbeke, Belgium) and medium was replaced after 24 h. Cell supernatant containing lentiviral vectors was collected on day 2 and 3 post-transfection and filtered through a 0.45 µm pore size filter (Sartorius, Minisart, Göttingen, Germany). Vector containing medium was concentrated by dissolving the vector pellet obtained by ultracentrifugation in 200 µl PBS. Functional vector titers were determined by transducing HEK-293T cells with the respective vector preparation in a 10-fold dilution series. Three days after transduction, cells were harvested, fixed in 4 % paraformaldehyde (PAF, VWR international prolabo, Leuven, Belgium) and analyzed using a FACSCalibur flow cytometer (BD Biosciences, Erembodegem, Belgium) and the CellQuest software package provided with the instrument. Functional vector titers are expressed as transducing units (TU) per ml (eGFP:2.5 E07 TU/ml and eGFP-LRRK2 G2019S: 4.0 E07 TU/ml). The lentiviral vector transfer construct for eGFP was previously described<sup>7</sup> and the LV transfer plasmid expressing eGFP-LRRK2 G2019S was derived from the previously described<sup>8</sup> LV-3flag-LRRK2 constructs in which the 3xFlag tag was replaced by an eGFP sequence. Lentiviral vectors (4µl) were injected unilaterally in the striatum of adult mice (4 mice per group, with one animal per group reserved for a negative control without staining, hence n=3 animals were used for the final counts) and perfused two weeks after injection, essentially as described<sup>9</sup>. Sections (50 µm) were stained for rabbit GLG1 (Sigma, 1:500), mouse GFP (Roche, 1:500), and Topro-3. Autofluorescence was quenched using 0.3% Sudan Black, in 70% ethanol, 10 min. Sections (2 sections per animal) were imaged using 63x objective using a Zeiss LSM510 confocal microscope. Each image represents average projection of seven z-stacks of 0.8 micron each. Approximately 20 cells per section were assessed for GLG1 staining in animals injected with eGFP-LRRK2 G2019S and 80 cells per section in animals injected with eGFP control.

### *Mass spectrometry*

Purified BAG5 WT and DARA mutant proteins were separated on 4-20 % SDS-PAGE, stained with Gelcode Blue Stain Reagent (Thermo Scientific). Individual bands were excised and digested with trypsin. Tryptic peptides were analyzed by a LC/MS/MS system with Finnigan Surveyor HPLC connected to Thermo LTQ XL mass spectrometer (Thermo Scientific). Protein identification was performed using MASCOT.

### *Protein purification and assays of Rab7L1 activity*

HEK293FT cells transfected with 3xFlag-Rab7L1 WT, T21N or Q67L plasmid DNAs were solubilized in lysis buffer containing 20 mM Tris-HCl pH 7.5, 150 mM NaCl, 1 mM EDTA, 1% Triton X-100, 10% Glycerol, 1x Halt phosphatase inhibitor cocktail (Thermo Scientific) and protease inhibitor cocktail (Roche) for 30 min on ice. Lysates were centrifuged (10 min, 20,000xg) and supernatants were precleared with EZview™ Red Protein G Affinity Gel (Sigma-Aldrich) for 30 min at 4°C then incubated with EZview™ Red ANTI-FLAG® M2 Affinity Gel (Sigma-Aldrich) for 1h at 4°C on a rotator. Proteins on beads were washed 6 times with 25 mM Tris-HCl pH 7.5, 400 mM NaCl, and 1% Triton X-100.

For binding assays, 3x-Flag-Rab7L1 fusion proteins bound to EZview™ Red ANTI-FLAG® M2 Affinity Gel (Sigma-Aldrich) were washed twice with Buffer A (20 mM Tris-HCl pH 7.5, 100 mM NaCl, 5 mM MgCl<sub>2</sub>, 1 mM NaH<sub>2</sub>PO<sub>4</sub>, 2 mM DTT) and incubated overnight on ice in Buffer A containing 0.1 μM <sup>32</sup>P-α-GTP. Beads were then washed twice in Buffer A to remove unbound nucleotides, added to the Bio-safe II (RPI) scintillation cocktail and binding quantified using scintillation counting for <sup>32</sup>P on an LS6500 scintillation counter (Beckman Coulter). Equal aliquots of beads with bound Rab7L1 proteins for WT, T21N or Q67L were collected for western blot analysis to estimate total protein loading.

To assay GTP/GDP retention, agarose-bound Rab7L1 proteins were incubated in Buffer A containing 0.1 μM [8-<sup>3</sup>H]-GTP or [8,5'-<sup>3</sup>H]-GDP overnight on ice and washed twice with Buffer A

to remove unbound nucleotide. Subsequently, proteins were incubated in Buffer A containing a 100-fold excess of unlabeled GTP or GDP for 0, 10, 20 or 30 min shaking at 37°C. After each time point, Rab7L1 proteins were washed twice with Buffer A, and retaining <sup>3</sup>H-GTP or <sup>3</sup>H-GDP bound to proteins was quantified using scintillation counting. The amount of <sup>3</sup>H-GTP or <sup>3</sup>H-GDP bound at 10, 20 and 30 min for each sample was calculated as a fraction of initial binding.

### *Co-Immunoprecipitation*

Cells were lysed in IP buffer: 20 mM Tris-HCl pH 7.5, 150 mM NaCl, 1 mM EDTA, 0.3% Triton X-100, 10% Glycerol, 1x Halt phosphatase inhibitor cocktail (Thermo Scientific) and protease inhibitor cocktail (Roche) for 30 min on ice. Lysates were centrifuged at 4°C for 10 minutes at 20,000 xg and supernatant further cleared by incubation with EZview™ Red Protein G Affinity Gel (Sigma-Aldrich) for 30 min at 4°C. For Flag tagged constructs, lysates were incubated with EZview™ Red ANTI-FLAG® M2 Affinity Gel (Sigma-Aldrich) for 1h at 4°C and eluted after six washes with wash buffer (20 mM Tris-HCl pH 7.5, 150 mM NaCl, 1 mM EDTA, 0.1% Triton X-100, 10% Glycerol) then eluted in 1x kinase buffer (Cell Signaling), containing 150 mM NaCl, 0.02% Triton and 150 ng/μl of 3xflag peptide (Sigma-Aldrich) with shaking for 30 mins at 4°C. GFP-tagged proteins were immunoprecipitated using GFP-nAb™ Agarose resin (Allele Biotechnology) and eluted after six washes with buffer as above by boiling in 4x NuPAGE LDS sample buffer (Invitrogen).

For tertiary IP, HEK293FT lysates were immunoprecipitated with anti-Flag monoclonal antibodies as described above. Equal aliquots of the first IP were collected for each sample (first IP) and eluates from the first IP were then used for the second IP with the Chromotek-GFP-Trap resin (Allele Biotechnology) for 30 min at 4°C. Beads were washed six times with IP wash buffer and immunoprecipitated complexes were eluted by boiling in 4x NuPAGE LDS sample buffer (Invitrogen).

### *SDS PAGE and Western Blotting*

Subcellular fractionation from HEK cell lysates was performed as previously described<sup>10</sup>. Other lysates were generated as described above.

Proteins were resolved on 4–20% Criterion TGX gels (Biorad) in SDS/Tris-glycine running buffer, and transferred to poly(vinylidene fluoride) (PVDF) membranes by semi-dry trans-Blot Turbo transfer system (Biorad) according to manufacturer's instructions. Membranes were blocked with 5% nonfat milk in Tris-buffered saline containing 0.1% Tween 20 (TBST) and then incubated for 1 hour at RT or overnight at 4°C with appropriate primary antibodies including: mouse anti-Flag M2 (Sigma-Aldrich, 1:5000); mouse anti-c-Myc, clone 9E10 (Roche, 1:2000); rabbit anti-LRRK2, MJF2 (Epitomics, 1:2000), rat anti-Hsc70 (Abcam, 1:2000); rabbit anti-BAG5 (Sigma, 1:2000); rabbit anti-14-3-3 (Santa Cruz Biotechnology, 1:2000); mouse anti-V5 (Invitrogen, 1:2000); mouse anti-GFP (Roche, 1:2000); mouse anti-GAK (MBL, 1:2000); rabbit anti-MEK1/2 (Cell Signaling, 1:5000); rabbit anti-Tom20 (Santa Cruz Biotechnology, 1:2000); rabbit anti-GM130 (Novus Biologicals, 1:2000); sheep anti-TGN46 (Serotec, 1:2000); gamma-adaptin (BD Transduction Laboratories, 1:2000); actin (Sigma, 1:5000); GST (GE Healthcare, 1:5000); CHIP (Santa Cruz, 1:200); 14-3-3 (Santa Cruz, 1:2000). Membranes were washed in TBST (3×5 min) at room temperature (RT) followed by incubation for 1 h at RT with horseradish peroxidase-conjugated anti-mouse or rabbit IgG (Jackson Immunoresearch Laboratories). Blots were washed in TBST (3×5 min) at RT, immunoreactive proteins were developed using enhanced chemiluminescence plus reagent (Thermo Scientific) and imaged on a STORM 860 Molecular Imager (GE).

### *Immunostaining*

Cells on coverslips were fixed with 4% paraformaldehyde in 1x PBS, blocked with 5% FBS in PBS with addition of 0.1% Triton. Primary antibodies were diluted in blocking buffer and incubated for 1 hour at RT. After three 5 min washes with PBS, secondary fluorescently labeled

antibodies (Invitrogen) were diluted in blocking buffer and were incubated for 1 hour at RT. Coverslips were then washed three times with PBS, stained for TOPRO-3 nuclear dye (Invitrogen) and mounted with The ProLong® Gold antifade reagent (Invitrogen). Primary antibodies used for ICC experiments included: mouse anti-Flag M2 (Sigma-Aldrich, 1:500); mouse anti-c-Myc, clone 9E10 (Roche, 1:500); sheep anti-c-Myc (Novus Biologicals, 1:500); rabbit anti-GM130 (Novus Biologicals, 1:200); sheep anti-TGN46 (Serotec, 1:200); rabbit anti-Flag (Sigma-Aldrich, 1:500); anti-V5 (Invitrogen, 1:500); mouse anti-LAMP1 (Developmental studies hybridoma bank, 1:250); rabbit anti-Mannose 6 phosphate receptor (M6PR; Abcam, 1:200); mouse anti-VPS35 (Abnova, 1:200); rabbit anti-GLG1 (Sigma, 1:300). All secondary antibodies used for ICC were from Invitrogen and have been used at 1:500: donkey anti-mouse Alexa Fluor® 488; donkey anti-rabbit Alexa Fluor® 568; donkey anti-sheep Alexa Fluor® 488; donkey anti-mouse Alexa Fluor® 647; donkey anti-mouse Alexa Fluor® 568; donkey anti-rabbit Alexa Fluor® 488.

### *Golgi morphology experiments*

For golgi morphology experiments, transfected cells or neurons were stained for trans-golgi markers TGN46 or GLG1. We used antibodies to TGN46 for human cell lines and GLG1 for mouse neurons and in mouse brain; this was because in our hands the TGN46 antibodies did not stain mouse tissue and, conversely, the GLG1 antibody gave no immunoreactivity in human cells. Cells were imaged on a Zeiss LSM510 Meta confocal using a 100x objective. Three Golgi phenotypes were identified: 1) Normal or diffused with multiple puncta throughout the cell; 2) Clustered or condensed with large golgi clusters, less than 3 clusters per cell; and 3) Cleared, with minimal or no golgi staining throughout the cell. Golgi morphology was counted in between 50-100 transfected cells per sample by an observer who was blinded to the transfection group (see below). Two or three independent experiments were performed and counts aggregated across experiments for a total of 100-300 cells per group.

### *Neurite length measurements*

Neurons were fixed in 4% PFA in PBS and stained with either mouse anti-Flag (clone M2, Sigma, 1:500), mouse anti-GFP or mouse anti-Myc (Roche, 1:300) along with either rabbit anti-MAP2 (Santa Cruz Biotechnology, 1:500) or chicken anti- $\beta$ III tubulin (Novus, 1:500). After washing, cells were then stained with anti-mouse-Alexa Fluor® 488 and anti-rabbit-Alexa Fluor® 568 (both at 1:500 dilution, Invitrogen). Coverslips were mounted using ProLong Gold (Invitrogen) and examined using a Zeiss LSM510 Meta microscope. Cells were identified by being positive for the appropriate neuronal marker and for transfected protein of interest in a blinded fashion (see below) and images collected along the length of the longest neurite. ImageJ software (<http://rsbweb.nih.gov/ij/download.html>) was used to determine the neurite length in mm, by tracing the length of the longest neurite from the center of the cells to the end of the neurite. Each experiment was repeated at least three times with independent batches of cells and transfections.

### *Reproducibility, blinding and statistical analyses*

For qualitative experiments, such as western blotting or immunoprecipitation, we repeated each experiment on a minimum of three independent occasions with independent batches of cells and transfections. For key results, e.g., confirmation of protein interaction by immunoprecipitation, results were confirmed by at least two individuals. Experiments based on counting immunostained cells, specifically counts of localization organellar morphology and neurite length, were performed in a blinded fashion. To achieve this, the individual performing the immunostaining mounted coverslips on glass slides labeled only with a numeric code for each cDNA construct. When cells were transfected or co-transfected, we used tagged control proteins (e.g., GFP or GUS) such that we measured only transfected cells in all conditions and that the blinded observer was not aware which slides represented negative control conditions. Codes were recorded and stored sealed, while a second

person performed the analysis. After counts or measurements were completed, numeric codes were replaced with identifiers for the cDNA construct prior to statistical analyses. Where possible, we set objective criteria for cell counts. Analysis of the human genetic data, including quality control parameters, were performed as described previously<sup>1,8</sup>.

All statistical analyses were performed using R<sup>1,9</sup>. For experiments with continuous measures comparing only two groups, we used two-tailed unpaired t-tests with Welch's correction for unequal variance. For experiments with continuous measures using more than one group and single explanatory variables, we used one-way ANOVA with Tukey's honest significant difference test *post hoc* to compare individual conditions if the overall  $p$  value was  $<0.05$ . For neurite length measurements, raw values were subjected to a log<sub>2</sub> transformation prior to analysis. Where two variables were included in the model, e.g., for time, we used two-way ANOVA. To compare proportions with more than two categories, we used Fisher's exact test on aggregate counts across experiments with a Bonferroni correction for the number of tests performed. To compare proportions of aligned reads between exome data and RNA-seq, we used Chi-Square test on the aggregate numbers of reads across heterozygous individuals.

### **Description of raw data tables**

Three text files are included that detail the output from Protoarray Prospector for two sets of experiments. The first two data files are from two batches of arrays probed with truncated, GST-tagged LRRK2. In the first data file, three conditions are compared – hybridization buffer alone, GST alone and GST-LRRK<sub>2970–2527</sub>. In the second data file, two conditions are compared, GST-LRRK<sub>2970–2527</sub> was incubated with either GDP or GMPPcP. For reference the GST image from the first hybridization batch is included in this file. The third data file includes two arrays that were hybridized in parallel with either Flag-tagged eGFP alone or Flag-tagged, full length LRRK2.

The upper three blocks of the files include details of the array files used; lot numbers of the arrays and detection wavelengths for fluorescence; and values for the control spots on each array.

The fourth block in each file has the following parameters:

Database ID, Ultimate ORF ID, Description (for file 3 only): Descriptive text for each recombinant protein on the array.

Block, Row, Column, Protein Amount: Location of protein spot on the array

File1 Hit: Flags for potential hits based on Z-score >3

File1 Signal.Used: Raw signal averaged from duplicate spots on the array

File1 Z-Factor : mean value Z-factor for all replicates of a given probe on this array

File1 Z-Score: Measure of the binding of a given protein relative to mean of all protein features on the array, in units of standard deviations

File1 CI P-Value: Greatest value Chebyshev's Inequality P-value for all replicates of a given probe on each array

File1 CV: Coefficient of variance for a probe on the array

File1 GenePix Flags: Inherited from GenePix

### Supplementary References

1. Civiero, L. *et al.* Biochemical characterization of highly purified leucine-rich repeat kinases 1 and 2 demonstrates formation of homodimers. *PLoS ONE* **7**, e43472 (2012).
2. Greggio, E. *et al.* The Parkinson disease-associated leucine-rich repeat kinase 2 (LRRK2) is a dimer that undergoes intramolecular autophosphorylation. *J. Biol. Chem.* **283**, 16906–16914 (2008).
3. Kalia, S. K. *et al.* BAG5 inhibits parkin and enhances dopaminergic neuron degeneration. *Neuron* **44**, 931–945 (2004).
4. Lee, D.-W., Wu, X., Eisenberg, E. & Greene, L. E. Recruitment dynamics of GAK and auxilin to clathrin-coated pits during endocytosis. *J. Cell. Sci.* **119**, 3502–3512 (2006).
5. McCoy, M. K., Kaganovich, A., Rudenko, I. N., Ding, J. & Cookson, M. R. Hexokinase activity is required for recruitment of parkin to depolarized mitochondria. *Hum. Mol. Genet.* (2013).doi:10.1093/hmg/ddt407
6. Jiang, M. & Chen, G. High Ca<sup>2+</sup>-phosphate transfection efficiency in low-density neuronal cultures. *Nat Protoc* **1**, 695–700 (2006).
7. Ibrahimi, A. *et al.* Highly efficient multicistronic lentiviral vectors with peptide 2A sequences. *Hum. Gene Ther.* **20**, 845–860 (2009).
8. Baekelandt, V. *et al.* Characterization of lentiviral vector-mediated gene transfer in adult mouse brain. *Hum. Gene Ther.* **13**, 841–853 (2002).
9. Daniëls, V. *et al.* Insight into the mode of action of the LRRK2 Y1699C pathogenic mutant. *J. Neurochem.* **116**, 304–315 (2011).
10. Lobbstaël, E. *et al.* Immunohistochemical detection of transgene expression in the brain using small epitope tags. *BMC Biotechnol.* **10**, 16 (2010).
11. Rudenko, I. N. *et al.* The G2385R variant of leucine-rich repeat kinase 2 associated with Parkinson's disease is a partial loss-of-function mutation. *Biochem. J.* **446**, 99–111 (2012).
12. International Parkinson Disease Genomics Consortium *et al.* Imputation of sequence variants for identification of genetic risks for Parkinson's disease: a meta-analysis of genome-wide association studies. *Lancet* **377**, 641–649 (2011).

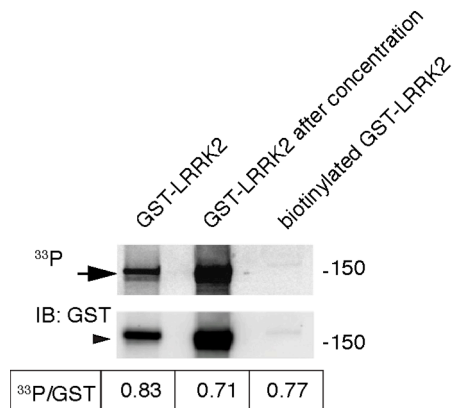


**Fig. S1. Biotinylated LRRK2 is kinase active.**

Truncated, GST-tagged LRRK2 (lane 1) was dialyzed and concentrated (lane 2) then biotinylated (lane 3) and subjected either to autophosphorylation and autoradiography (upper panel) or blotting for GST (lower panel). Autophosphorylation was detected in all samples; ratios of  $^{33}\text{P}$  to GST are shown below each lane. Data is representative of duplicate biotinylation experiments. Markers on the right of each panel are in kilodaltons.

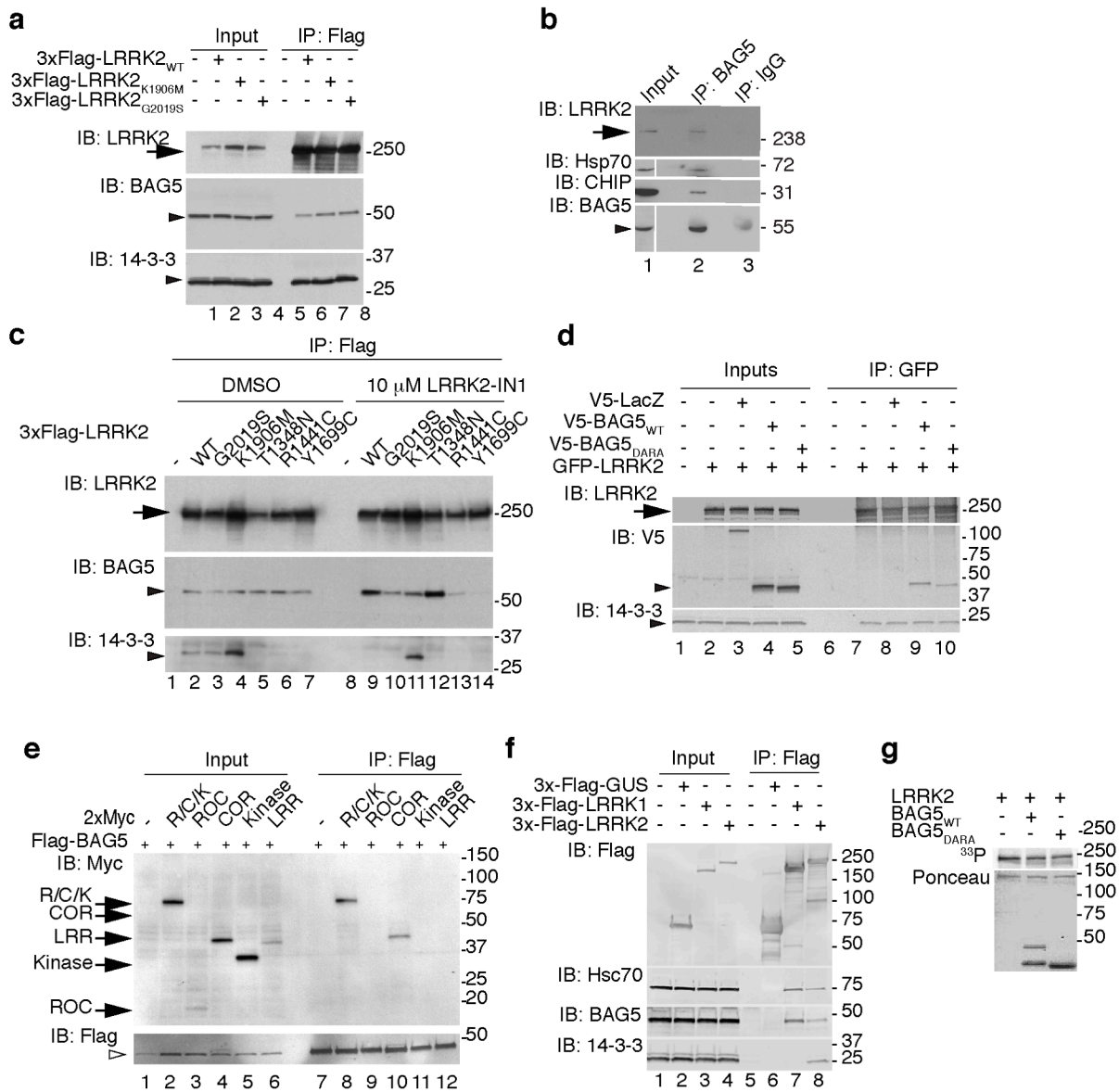


**Fig. S2. Additional co-immunoprecipitation data for BAG5**

**(a)** LRRK2 variants interact with BAG5. Cells lines stably expressing Flag-tagged LRRK2 variants were lysed and subjected to immunoprecipitation with FLAG-beads and probed for LRRK2 (top blot), BAG5 (middle) or 14-3-3 proteins (lower blot) as a positive control for LRRK2 interaction. Vector only cells are a negative control, shown in the first and fifth lanes.

**(b).** Endogenous LRRK2 and BAG5 were co-immunoprecipitated from mouse brain.

**(c).** BAG5 interaction is independent of LRRK2 kinase activity. Stable HEK293 cell lines expressing indicated Flag-tagged LRRK2 variants were treated with DMSO or 10 mM LRRK2-IN-1. Immunoprecipitated complexes were blotted for LRRK2 (upper panel), endogenous BAG5 (middle panel) or endogenous 14-3-3 proteins (lower panel).

**(d,e).** Sequence requirements. (d) V5-tagged WT or DARA mutant BAG5 (closed arrowheads) co-immunoprecipitated with GFP-tagged LRRK2. (e) Myc tagged domain constructs for LRRK2 co-immunoprecipitated with Flag-tagged BAG5 (closed arrowhead). R/C/K is ROC/COR/kinase.



**(f).** BAG5 interacts with LRRK1 and LRRK2. Immunoprecipitated complexes from cells expressing Flag-tagged GUS, LRRK1 or LRRK2 were blotted sequentially for Flag, BAG5, Hsp70 or 14-3-3 (from top to bottom). Inputs are shown in lanes 1-4 and immunoprecipitated complexes in lanes 5-8.

**(g)** Addition of BAG5 does not alter LRRK2 autophosphorylation. Full length LRRK2 was subjected to autophosphorylation reaction in vitro (upper panel showing  $^{33}\text{P}$ ) either alone (lane 1) or in the presence of wild type (lane 2) or DARA mutant (lane 3) BAG5. Lower panel shows Ponceau staining of the membrane for loading.

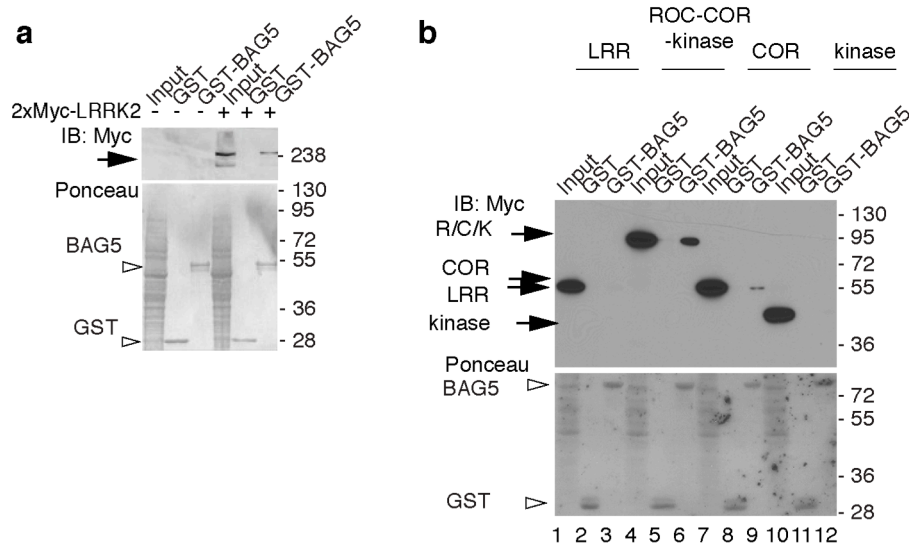


**Fig. S3. GST pull-downs as an additional validation technique.**

**(a)** GST-pull-downs confirm BAG5 interaction with LRRK2. Lysates from cells expressing myc-tagged LRRK2 were subjected to GST pull-downs with GST alone or GST-BAG5. Upper panel shows Myc blot, lower panel shows Ponceau staining for total lysates and GST fusion proteins.

**(b)** Pull-downs were performed with GST or GST-BAG5 from cells transfected with myc tagged LRRK2 domain constructs. Immunoprecipitates were blotted for Myc (upper panel) or stained with Ponceau (lower panel) to show equal loading.

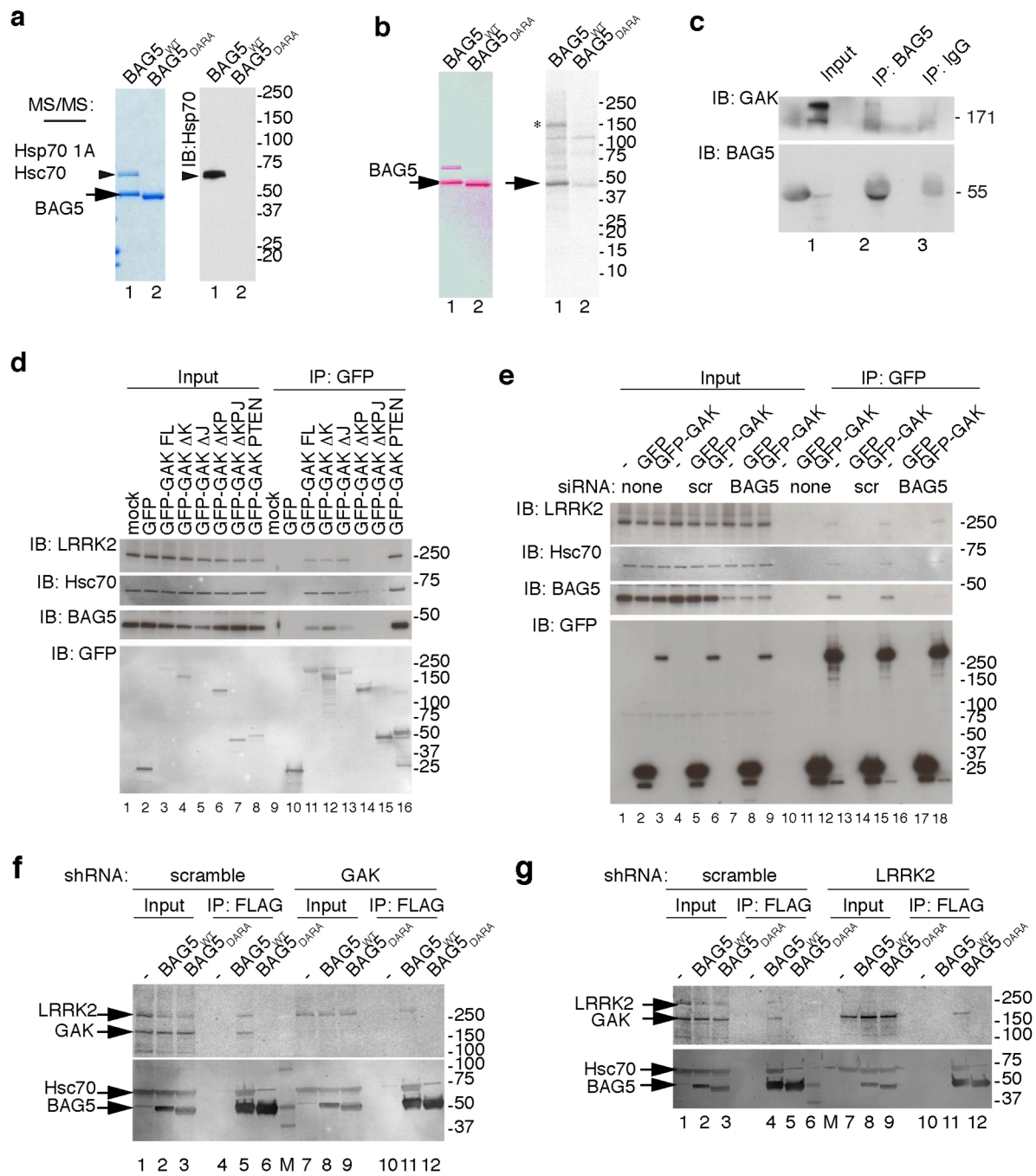


**Fig. S4. Additional protein interaction data for BAG5, GAK and Rab7L1**

(a) Purification of BAG5. Wild type BAG5 (lane 1) or DARA mutant (lane 2) were purified using Flag immunoprecipitation and complexes stained with Coomassie blue. Proteins in the upper band at ~70 kDa were isolated from this gel and identified by mass-spectrometry. Right panel shows a western blot using anti-Hsp70.

- (b)** A copurified kinase in preparations of wild type BAG5. Flag-purified WT or DARA- BAG5 were visualized with Ponceau-S staining (left panel) or subjected to autoradiography after incubation with kinase assay buffer and  $^{32}\text{P}$ -ATP (right panel). Arrow indicates BAG5 and the asterisk shows an ~150 kDa autophosphorylated kinase.
- (d)** BAG5 and LRRK2 both bind to the PTEN-like domain of GAK. Immunoprecipitated complexes with GFP-tagged GAK domains probed for endogenous LRRK2, Hsc70 and BAG5.
- (c)** Endogenous BAG5 and GAK interact *in vivo*. Mouse brain samples co-immunoprecipitated for BAG5 and probed for endogenous GAK (upper panel) and BAG5 (lower panel). IgG is a negative control.
- (e)** Knockdown of BAG5 does not disrupt interactions between GAK and LRRK2. HEK cells were co-transfected with scrambled siRNA or siRNA against BAG5 with no additional plasmids, GFP or GFP-GAK. Inputs (lanes 1-9) and samples after immunoprecipitation (lanes 10-18) were blotted sequentially for endogenous LRRK2, Hsc70, and BAG5 as well as transfected GFP proteins.
- (f)** Lack of GAK does not prevent LRRK2 from interacting with BAG5. HEK293FT cells stably expressing control shRNA or shRNA against GAK were transfected with Flag-vector, WT or DARA mutant BAG5. Lysates (lanes 1-3 and 7-9) and complexes immunoprecipitated with antibodies to Flag (lanes 4-6 and 10-12) were blotted with antibodies to LRRK2 and GAK (upper panel) and BAG5 and Hsc70 (lower panel). The middle lane (M) shows markers.
- (g)** Lack of LRRK2 does not prevent GAK from interacting with BAG5. HEK293FT cells stably expressing control shRNA or shRNA against LRRK2 were transfected with Flag-vector, WT or DARA mutant BAG5. Lysates (lanes 1-3 and 7-9) and complexes immunoprecipitated with antibodies to Flag (lanes 4-6 and 10-12) were blotted with antibodies to LRRK2 and GAK (upper panel) and BAG5 and Hsc70 (lower panel).

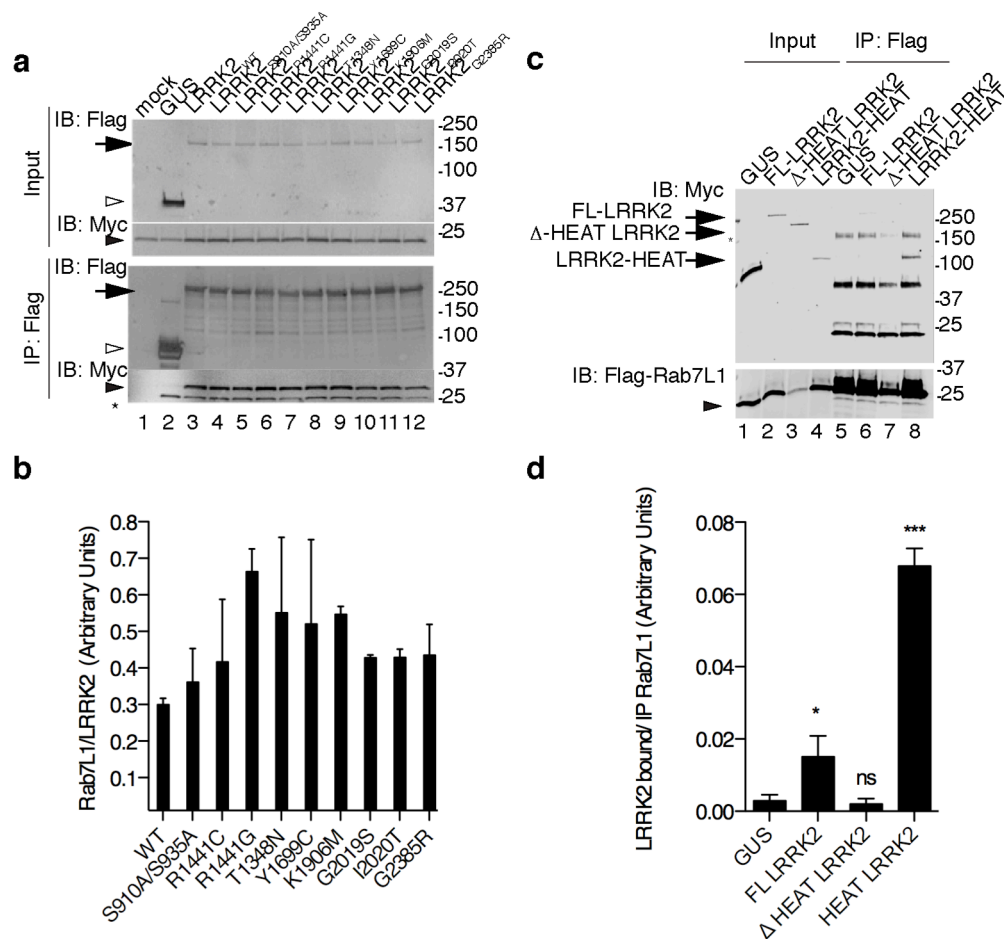


**Fig. S5. Mapping of interaction of Rab7L1 to LRRK2.**

**(a)** Binding between WT Rab7L1 and LRRK2 mutants was assessed by co-immunoprecipitation of Myc-tagged Rab7L1 with the indicated Flag-tagged LRRK2 variants. Upper panel shows inputs for Flag and Myc, lower panels show samples after immunoprecipitation probed for Flag (asterisk in the lower Myc blot shows a cross-reactive band of unknown identity).

**(b)** Quantification was performed by comparing the amount of Rab7L1 to the amount of LRRK2 in the IP. There were no significant differences between variants ( $F(9,19)=0.639$ ,  $p=0.751$  by one-way ANOVA,  $n=3$  independent experiments). Molecular weight markers on the right of all blots are in kilodaltons.

**(c)** Rab7L1 binds to the HEAT domain of LRRK2. Tagged (3xFlag) Rab7L1 immunoprecipitates full length 2xMyc-LRRK2 (upper blot, lane 6) and 2xMyc-HEAT domain of LRRK2 (upper blot, lane 8), but not 2xMyc-gus (upper blot, lane 5) and diminishes binding to 2xMyc-deltaHEAT LRRK2 (upper blot, lane 7). Lysates are shown in lanes 1-4 (upper blot). Samples were blotted for Flag (lower blot) to show immunoprecipitated Rab7L1.

**(d)** Quantifications for (c) were performed by estimating the ratio between immunoprecipitated LRRK2 to the levels of LRRK2 in inputs. Differences in interaction strength were analyzed by one-way ANOVA for all variants with Tukey's HSD post-hoc test compared to GUS negative control (\*,  $p<0.05$ ; \*\*\*,  $p<0.001$ ; ns = not significant;  $n=3$  independent experiments).

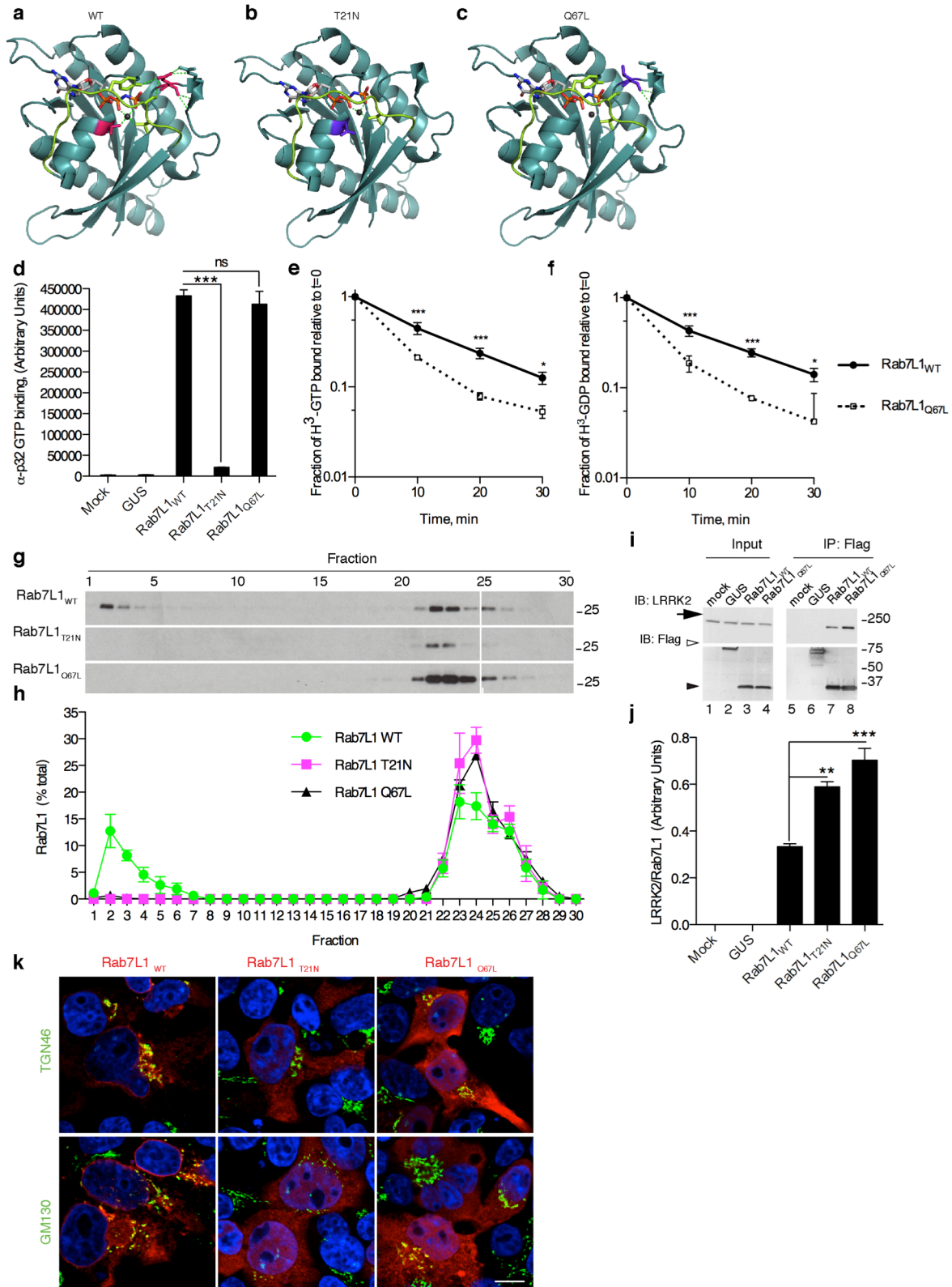


Fig. S6. Characterization of Rab7L1 mutants.

**(a-c)** Structural model of wild type Rab7L1 (a) showing key residues around the bound non-hydrolysable GTP analog, GppNHP that were mutated to influence function. These include a mutation that should disrupt  $Mg^{2+}$  co-ordination, T21N (b); and a key base for co-ordination and hydrolysis of GTP, Q67L (c).

**(d)** GTP binding for all variants was measured by loading with radiolabelled GTP and is normalized to total protein loading estimated by western blotting. Each bar represents the mean and SEM between four independent experiments. Statistical significance was estimated by one-way ANOVA with Tukey's *post-hoc* test; \*\*\*,  $p < 0.001$ .

**(e, f)** Guanosine nucleotide retention assays. Rab7L1 WT (solid lines) or Q67L (dashed lines) were loading with radiolabelled GTP (e) or GDP (f) and retention measured as a fraction of initial binding (y axes) as times up to 30 minutes (x axes). Each point is the mean and SD from three independent experiments. Statistical significance was estimated by two-way ANOVA for time versus mutation with Tukey's *post-hoc* test for comparison to wild type protein at each time point (\*\*,  $p < 0.01$ ; \*\*\*,  $p < 0.001$ ).

**(g,h)** Cell lysates were separated by size exclusion chromatography from highest to lowest retention time (fractions 1-30) and blotted for Flag-tagged Rab7L1 with (from top to bottom) the WT, T21N or Q67L variants. Quantification across  $n=3$  independent experiments (h) showed accumulation in early fractions for WT Rab7L1 but not T21N or Q67L.

**(i,j)** Interaction of LRRK2 with Rab7L1 is increased with guanosine nucleotide binding deficient Rab7L1 mutations. HEK293FT cells were transfected with Flag-tagged b-glucuronidase (GUS) or WT or Q67L Rab7L1 were immunoprecipitated for Flag and blotted for endogenous LRRK2 (upper blots) or transfected Flag-tagged proteins (lower panels). Markers on the right of the blots are in kilodaltons. Quantification **(j)** of the amount of LRRK2 relative to Rab7L1 in the immunoprecipitated complexes was performed for the indicated variants and statistical analysis performed using one-way ANOVA with Tukey's *post hoc* test ( $n=3$  independent experiments; \*\*\*,  $p < 0.001$  vs. WT Rab7L1).

**(k)** WT but not mutant Rab7L1 localizes to the trans-Golgi. Cells were transfected with WT (upper panels), T21N (middle panels) or Q67L (lower panels) Rab7L1 (red) and stained with two golgi markers (green), GM130 (left panels) or TGN46 (right panels). Cells were counterstained with TOPRO-3 to show the nucleus (blue in all images). Scale bar indicates 10  $\mu$ m.

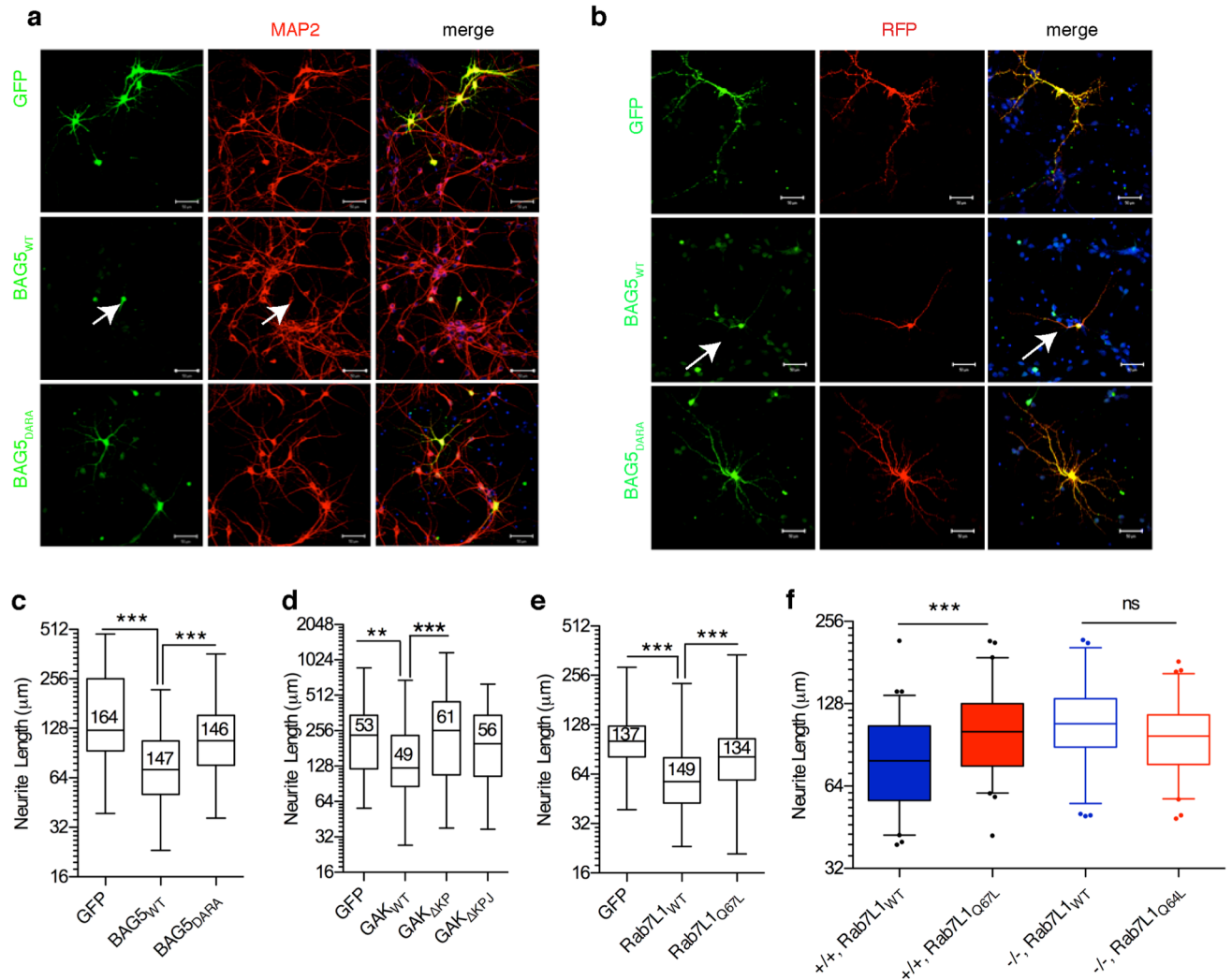


**Fig. S7. Neurite shortening phenotypes and expression of LRRK2 binding partners**

**(a,b)** Representative images of neurite length in BAG5 transfected neurons. **(a)** Primary neurons transfected with GFP, WT or DARA BAG5, stained with GFP or BAG5 (green) and MAP2 (red). Scale bars represent 50 μm. **(b)** Primary cortical neurons co-transfected with RFP and either GFP (upper panels), wild type BAG5 (middle panels) or the Hsp70-deficient DARA mutant (lower panels) and stained with GFP or BAG5 (left panels, green in merge) and RFP. Right panels show merged images with nuclear staining (blue). Scale bars represent 50 μm.

**(c-e)** Neurite length was measured in transfected neurons for BAG5 **(c)**, GAK **(d)** and Rab7L1 **(e)** constructs. Numbers in each box are the number of cells measured across 2-3 independent cultures. \*\*,  $p < 0.01$ ; \*\*\*,  $p < 0.001$  by one-way ANOVA with Tukey's *post-hoc* test compared to WT after log(2) transformation.

**(f)** Quantitation of neurite length per cell in transfected cells shows a significant difference in neurite length for WT Rab7L1 in with type (+/+) neurons but not in LRRK2 knockout (-/-) neurons. \*\*\*= $p < 0.0001$ ; ns=not-significant; compared to WT Rab7L1 for the same genotype.

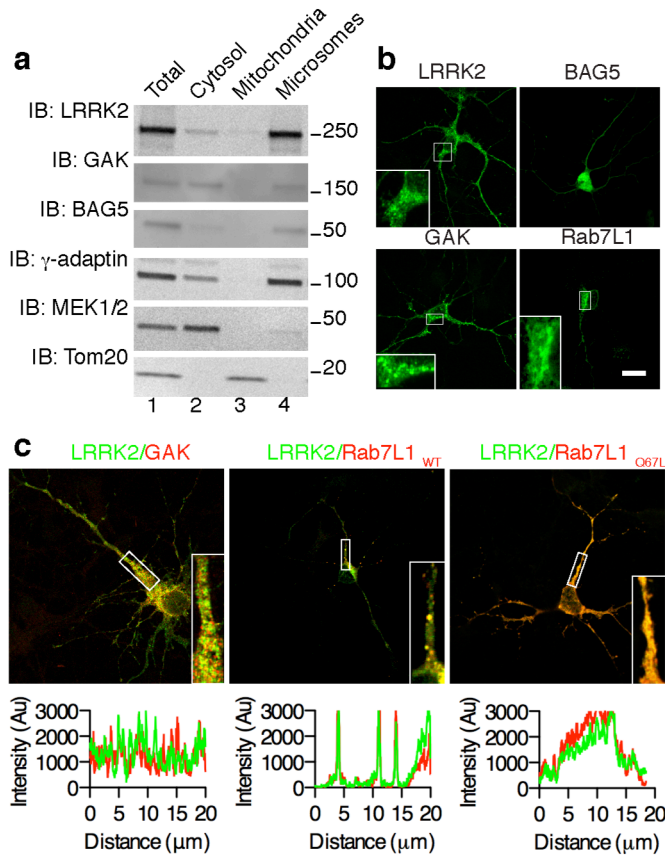


**Fig. S8. LRRK2 complex components co-localize to vesicular compartments of neurons**

(a) Subcellular fractionation. Lysates (lane 1) from HEK293FT cells transfected with Flag-tagged LRRK2 were separated into cytosolic (lane 2), mitochondrial (lane 3) and microsomal (lane 4) fractions and blotted for endogenous proteins. Markers on the right of the blots are in kilodaltons.

(b) Localization of tagged proteins in neurons. Insets show examples of vesicular staining for LRRK2, GAK and Rab7L1. Scale bar indicates 10  $\mu$ m.

(c) Colocalization of LRRK2 with GAK or Rab7L1 in neurons. Flag-tagged LRRK2 was co-transfected with myc-tagged GAK, WT or Q67L Rab7L1. Insets show vesicular structures and plots below each image are of staining intensity.



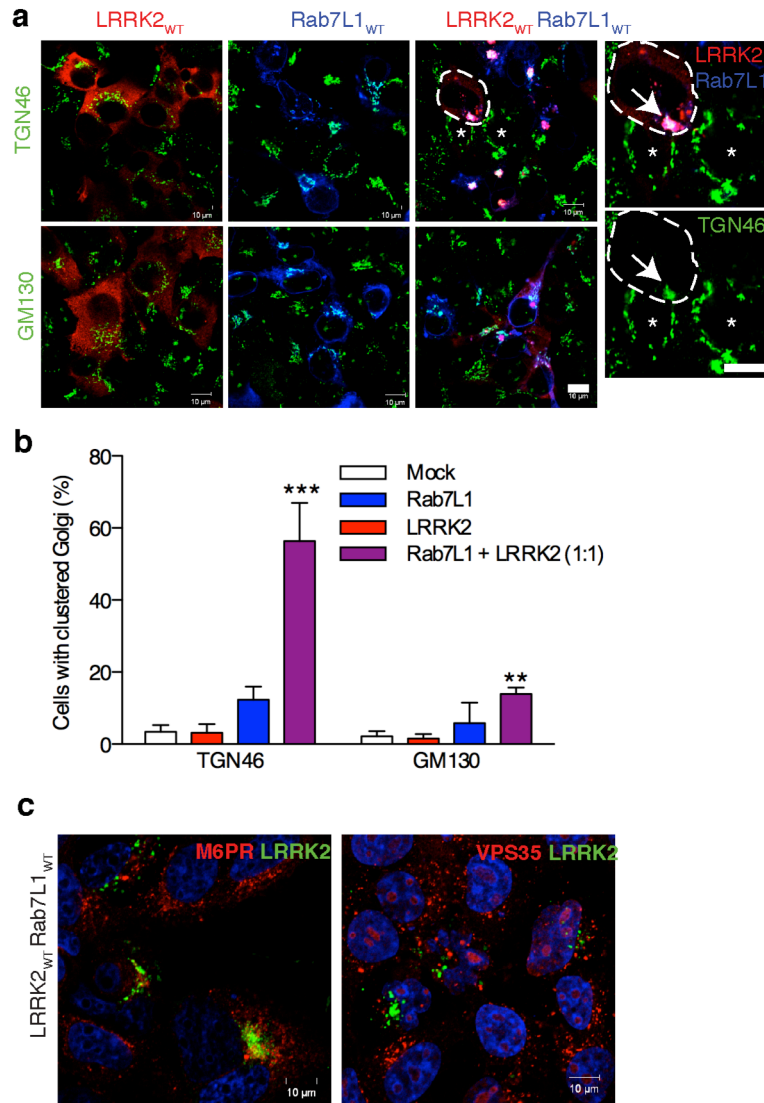


**Fig. S9. Additional data related to clustering and clearance of Golgi.**

**(a)** LRRK2 (red) and Rab7L1 (blue) in transfected alone or together into HEK cells that were stained for the trans-Golgi marker TGN46 (green, upper panels) or the cis-Golgi marker GM130 (green, lower panels). Note partial colocalization with GM130 but stronger colocalization with TGN46, which also shows disrupted morphology when the two proteins are cotransfected. Panels on the right show an enlarged cell, outlined, with clustered TGN46 staining that is also positive for Rab7L1 and LRRK2 (upper panel; lower panel shows TGN46 alone). Two adjacent cells that were not co-transfected are also shown with normal TGN46 staining (asterisks). Scale bar indicates 10 mm.

**(b)** These effects were quantified by counting cells with relocation of LRRK2 and statistical analysis performed using one-way ANOVA with Tukey's *post hoc* test ( $n=3$  independent experiments with 100 cells counted per experiment; \*\*,  $p<0.01$ ; \*\*\*,  $p<0.001$  vs. WT Rab7L1 for each marker separately).

(c) LRRK2 positive structures (green) in cells co-transfected with LRRK2 and Rab7L1 do not colocalize with retromer markers (red) including the cation-independent mannose-6-phosphate receptor (M6PR, left image) or VPS35 (right image). Scale bars indicate 10  $\mu$ m.

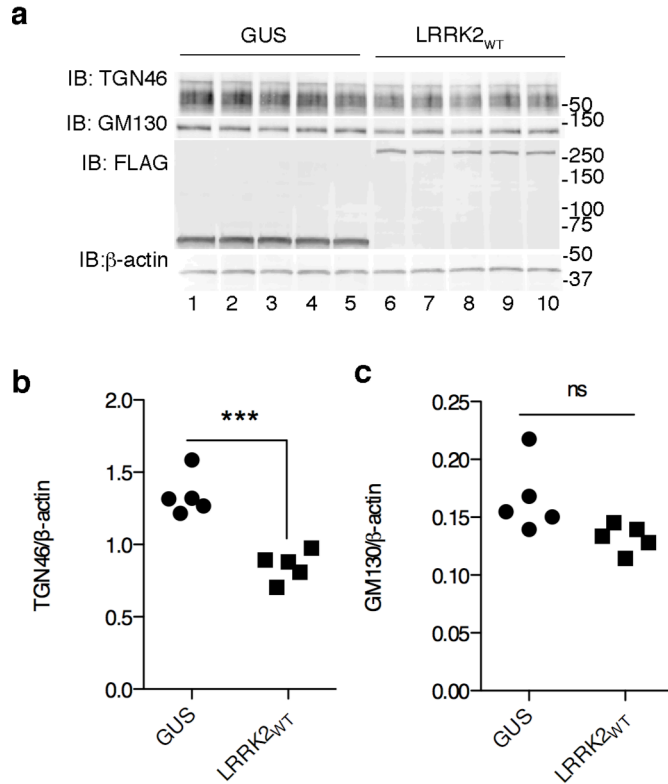


**Fig. S10. Biochemical confirmation of turnover of trans-Golgi.**

(a) Western blot to confirm turnover of TGN46, but not GM130, in LRRK2 transfected cells. Cells were transfected with Flag-tagged GUS (lanes 1-5) or LRRK2 (lanes 6-10). Twenty-four hours after transfection, cell lysates were blotted sequentially for TGN46, GM130, FLAG for transfected proteins and  $\beta$ -actin as loading control. Markers on the right are in kilodaltons.

(b,c) Graphs show ratio of TGN46 to  $\beta$ -actin (b) or GM130 to  $\beta$ -actin (c) from  $n=5$  individual transfections. \*\*\*,  $p < 0.001$ ; ns, not significant ( $p = 0.07$ ), two sample t-test with Welch's correction for unequal variance. Representative of duplicate independent experiments with similar sample numbers.

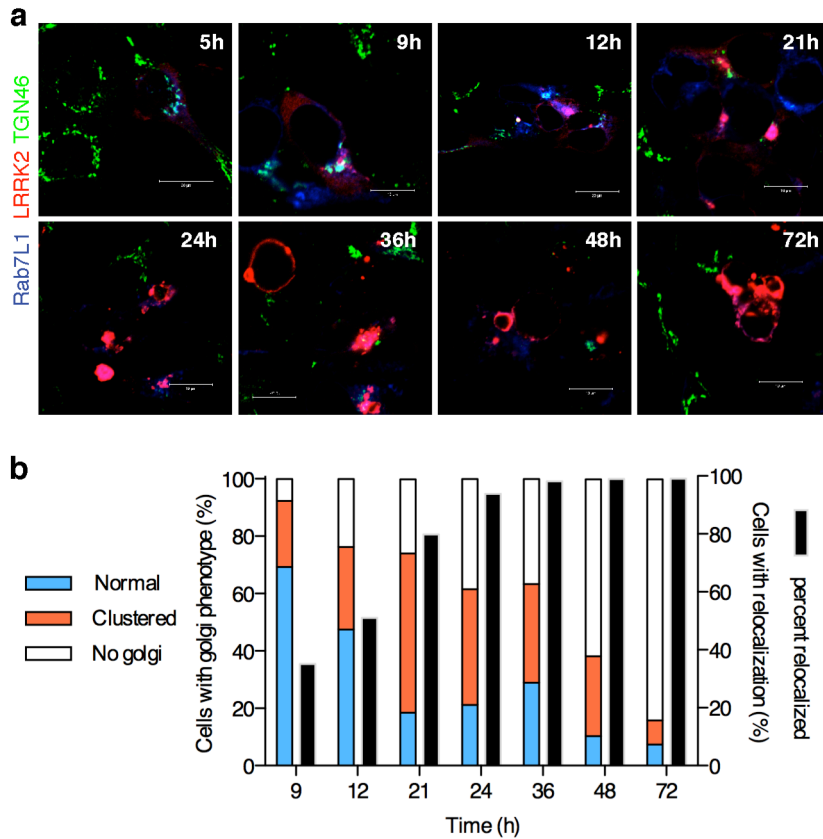


**Fig. S11. Time course of recruitment of LRRK2 to, and clearance of, the trans-Golgi network.**

**(a)** Cells were transfected with LRRK2 and Rab7L1 and imaged after staining for TGN46 (green) at the indicated times after transfection.

**(b)** Blinded counts (proportions on the left y-axis) of cells with normal Golgi (blue), clustered Golgi (orange) or cells with minimal or no apparent Golgi stained (white) at the times indicated on the x-axis. Recruitment of LRRK2 was also scored in the same cells (black bars).

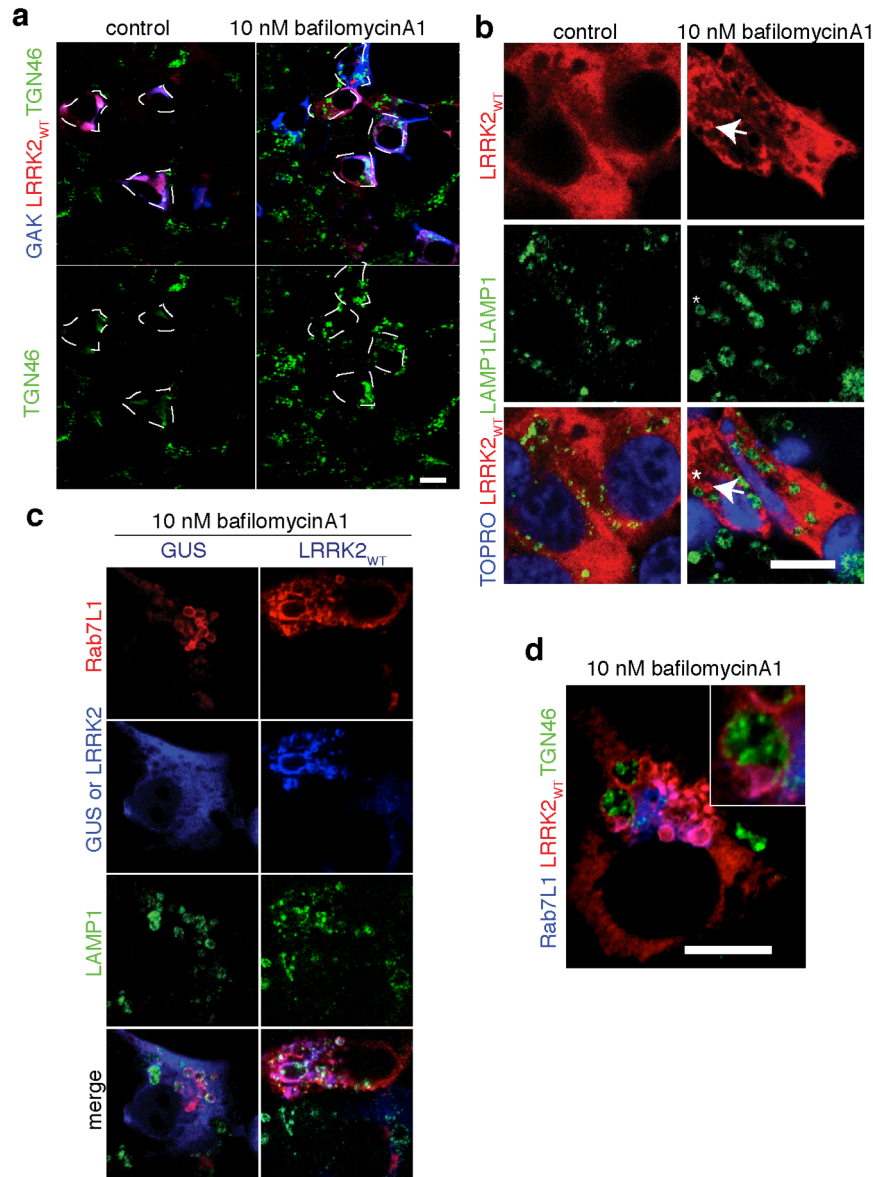


**Fig. S12. Additional data related to mechanism of Golgi turnover by lysosomes**

**(a)** Bafilomycin A1 prevents turnover of TGN-46 vesicles in the presence of LRRK2 with GAK. Cells were co-transfected with LRRK2 and GAK and treated with DMSO (left panels) or 10nM bafilomycin A1 (right panels). Upper panels show staining for LRRK2 (red) and GAK (blue) to identify co-transfected cells (indicated by outlines), lower panels show only TGN46 stain in the same cells.

**(b)** Effect of bafilomycin A1 on relative localization of LRRK2 and lysosomes.

Cells expressing wild type LRRK2 were treated with DMSO (control; left panels) or 10 nM bafilomycin-A1 (right panels) for 24h and stained for LRRK2 (red, upper panels) and LAMP1 (green, middle panels). After bafilomycin-A1 treatment, vesicles containing LRRK2 (arrow) are seen adjacent to LAMP1-positive lysosomes (asterisk).

**(c)** LRRK2/Rab7L1 vesicles surround lysosomes after bafilomycin-A1 treatment. Cells were transfected with GUS (left) or LRRK2 (right) and treated with 10 nM bafilomycin-A1 for 24h, then stained for Rab7L1 (red), LRRK2 (blue) and LAMP1 (green; merged images are shown in the bottom set of panels).

**(d)** LRRK2 vesicles engulf trans-Golgi. Cells expressing LRRK2 (red) with Rab7L1 (blue) were treated with bafilomycin A1 (10 nM, 24h) and stained with TGN46 (green). Scale bars represent 10  $\mu$ m.

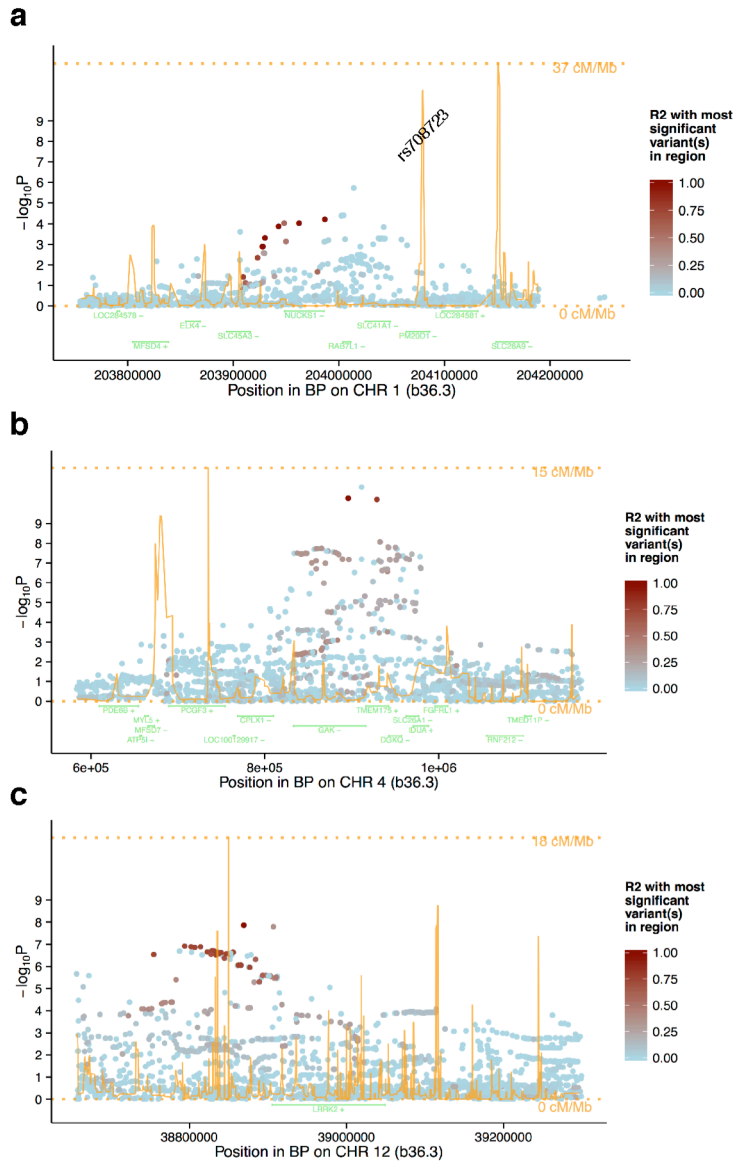


**Fig. S13. Additional human genetic data.**

Locus plots for PD risk for markers around Rab7L1/PARK16 (a), GAK (b) or LRRK2 (c) showing markers on the x-axes against  $-\log_{10}$  of  $p$  values for association with PD risk (y axes). Each point is colored by strength of linkage disequilibrium with the most highly significant marker in the region. The orange line shows recombination rate in centimorgans and positions of known genes in the region are shown below the plot in green.

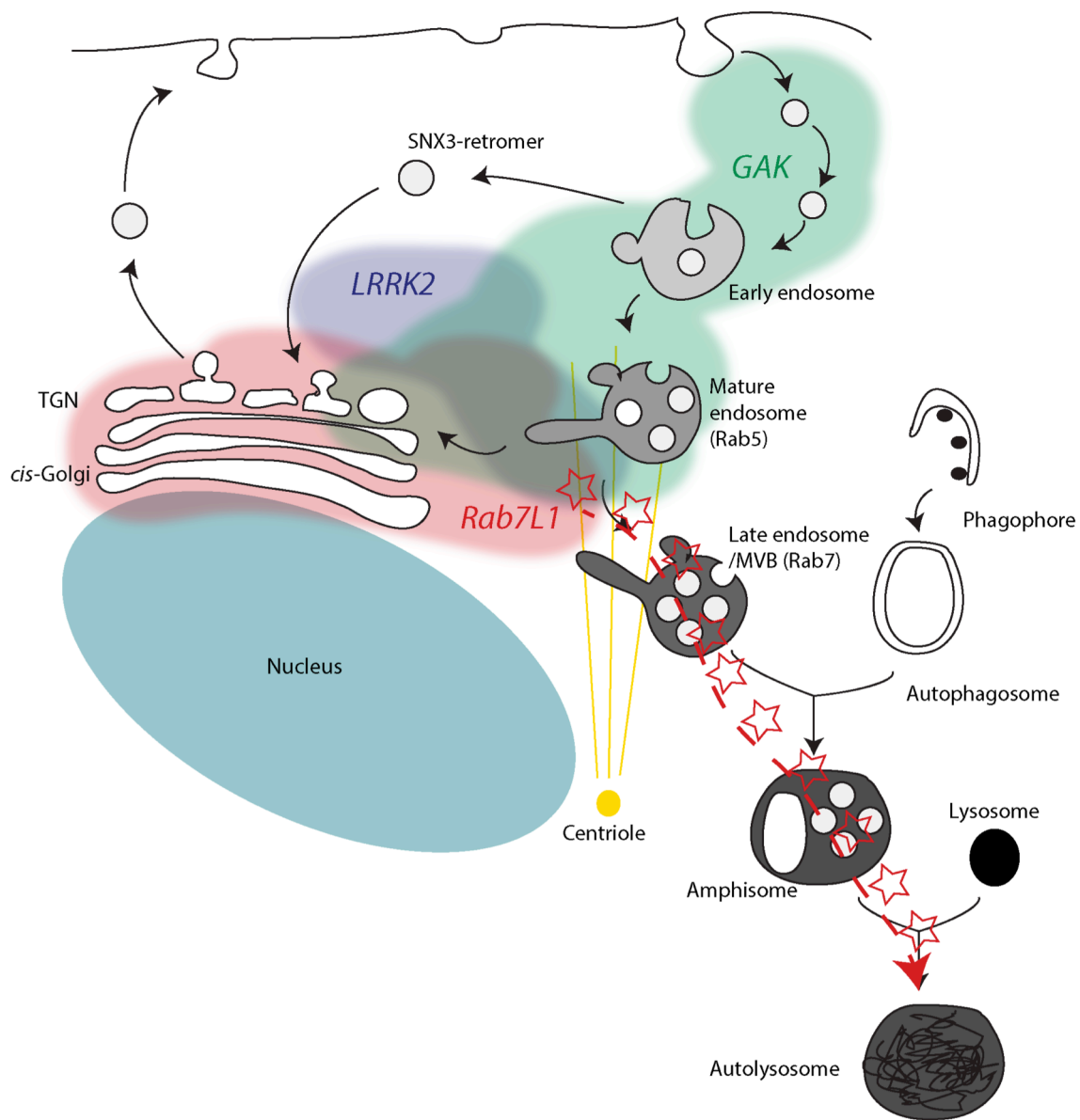


**Fig. S14. Proposed model for LRRK2 complex formation and role in turnover of TGN**

Schematic of major vesicular sorting pathways within a mammalian cells showing secretory pathway from the TGN and endocytosis from the plasma membrane. Overlaid on this schematic are our proposed regions of localization of LRRK2 (blue), GAK (green) and Rab7L1 (red), suggesting co-complex formation around the TGN and mature endosomes. Once formed, this complex helps traffic golgi-derived vesicles through the autophagy-lysosomal system. Adapted in part from models in Cullen and Korswagen<sup>12</sup> and from data in<sup>13</sup>

**Table S1 Candidate protein interactors for truncated LRRK2<sup>1</sup>**

Database ID	Name	Gene symbol	Z score				
			Buffer	GST	GST-LRRK2	GST-LRRK2 + GDP	GST-LRRK2 + GMP PcP
BC050551	BCL2-associated athanogene 5	BAG5	-0.001	0.6394	31.33	68.41	45.99
BC020221	SH3 and cysteine rich domain	STAC	0.161	2.785	15.66	3.754	3.626
NM_004281	BCL2-associated athanogene 3	BAG3	-0.062	-0.073	14.95	23.95	16.97
NM_006819	Stress-induced-phosphoprotein 1 (Hsp70/Hsp90-organizing protein)	STIP1	-0.574	2.078	10.90	24.27	26.56
NM_153498	Calcium/calmodulin-dependent protein kinase	CAMK1D	-0.113	2.135	8.137	4.873	3.934
BC036089	Myeloid/lymphoid or mixed-lineage leukemia	MLLT3	-0.005	0.5998	5.139	4.485	7.208
NM_004282	BCL2-associated athanogene 2	BAG2	-0.232	-0.222	3.555	10.25	7.602
BC056415	RNA polymerase II associated protein 3	RPAP3	-0.214	2.632	3.075	3.024	4.694

<sup>1</sup>Candidate interactors were filtered where Z>3 for LRRK2 in all experiments and <3 for GST and buffer



**Table S2 Candidate protein interactors for full length LRRK2**

Database ID	Name	Gene symbol	Z score	
			GFP	LRRK2
NM_003406.2	tyrosine 3-monooxygenase/tryptophan 5-monooxygenase activation protein, zeta polypeptide	YWHAZ	-0.02109	14.04168
NM_017949.1	CUE domain containing 1	CUEDC1	0.83579	12.31015
NM_004281.2	BCL2-associated athanogene 3	BAG3	1.30739	10.81284
BC068456.1	14-3-3 protein zeta/delta	YWHAZ/D	-0.29605	9.93861
NM_003404.2	tyrosine 3-monooxygenase/tryptophan 5-monooxygenase activation protein, beta polypeptide	YWHAB	0.62477	8.46554
NM_004282.2	BCL2-associated athanogene 2	BAG2	0.12599	7.64759
NM_006142.1	stratifin	SFN	0.08443	7.21162
PV3502	p21(CDKN1A)-activated kinase 6	PAK6	1.06919	6.71068
BC015818.1	lectin, galactoside-binding, soluble, 8 (galectin 8)	LGALS8	1.92125	6.22942
NM_004873.1	BCL2-associated athanogene 5	BAG5	0.36259	5.45035
NM_006007.1	zinc finger, AN1-type domain 5	ZFAND5	2.41843	5.33141
PHC1695	C-X-C motif chemokine 11	CXCL11	2.68541	4.87759
NM_145010.1	chromosome 10 open reading frame 63	C10orf63	0.56561	4.44299
NM_012148.1	double homeobox, 3	DUX3	0.2267	4.32587
NM_012387.1	peptidyl arginine deiminase, type IV	PADI4	0.88694	4.29751
XM_379498.2	PREDICTED: Homo sapiens hypothetical LOC401363	LOC401363	1.52639	4.12505
NM_144736.3	Protein midA homolog, mitochondrial	NDUFAF7	2.3465	4.08204
NM_018270.3	MRG-binding protein	MRGBP	1.81255	4.01571
BC053836.1	Vasohibin-2	VASH2	1.93405	3.96401
NM_181526.1	myosin, light chain 9, regulatory	MYL9	1.57116	3.96127
BC050551.1	BCL2-associated athanogene 5	BAG5	0.44732	3.90867
BC008668.1	cyclin G associated kinase	GAK	1.15871	3.90226
BC047776.2	coiled-coil domain containing 43	CCDC43	1.2882	3.72293
BC022888.1	xin actin-binding repeat containing 2	CMYA3	0.53045	3.62777
NM_001819.1	chromogranin B (secretogranin 1)	CHGB	0.65034	3.62686
BC002914.1	WAS/WASL-interacting protein family member 1		2.09232	3.55733

NM_003929.1	RAB7, member RAS oncogene family-like 1	RAB7L1	1.16831	3.48276
BC007067.1	Kinetochores-associated protein NSL1 homolog	NSL1	1.67187	3.46034
BC006177.1	Metastasis-associated protein	MTA1	1.19548	3.44433
NM_004092.2	Enoyl-CoA hydratase, mitochondrial	ECHS1	1.6383	3.43609
BC014774.1	BCL2-associated athanogene	BAG1	0.45691	3.43015
NM_025104.2	Protein DBF4 homolog B	DBF4B	1.83174	3.37113
NM_014904.1	RAB11 family interacting protein 2 (class I)	RAB11FIP2	1.24823	3.37022
BC035026.2	family with sequence similarity 47, member B	FAM47B	1.03882	3.33362
BC002369.1	Serine/threonine-protein kinase	PLK1	2.71898	3.20003
NM_032017.1	serine/threonine kinase 40	STK40	1.0596	3.13874
BC032347.1	chromosome 8 open reading frame 59	C8orf59	1.56636	3.1241
PV4202	NIMA (never in mitosis gene a)-related kinase 1	NEK1	1.20667	3.08887
NM_005659.1	ubiquitin fusion degradation 1 like (yeast)	UFD1L	1.85731	3.07149
NM_138558.1	protein phosphatase 1, regulatory (inhibitor) subunit 8	PPP1R8	0.815	3.01796
PV3370	megakaryocyte-associated tyrosine kinase	MATK	1.54718	3.00607
NM_005861.2	STIP1 homology and U box-containing protein 1	STUB1	-0.18894	2.94248

<sup>1</sup>Candidate interactors were filtered where Z>3 for LRRK2 and <3 for GFP